# A COMPUTER SIMULATION STUDY OF COMPRESSOR TUNING PHENOMENA

J. J. NIETER AND R. SINGH

*Department of Mechanical Engineering, The Ohio State University, Columbus, Ohio* 43210, *U.S.A.*

(*Received* 10 *November* 1983, *and in revised form* 27 *February* 1984)

Basic thermofluid processes of a positive displacement compressor are strongly dependent upon the acoustic behavior of the manifolds. The tuning process of such a compressor is fairly complex as increases in the mass flow rate may not correspond with higher energy efficiencies. In this paper a computer simulation program is described, which includes the manifold back pressure effect, developed to investigate and explain the tuning phenomena for a single or two-cylinder reciprocating compressor. A symmetric suction manifold system for a two-cylinder refrigeration compressor has been considered as the example case in this tuning study. Results for flow efficiency, energy efficiency, and pressure pulsations at the valve exit are presented in terms of the acoustic natural frequencies of the manifold system. Predicted results compare reasonably well with experimental data. Based on this study, it is possible to choose optimal manifold dimensions which will provide higher efficiencies with lower pressure pulsations.

## 1. INTRODUCTION

The idea of tuning positive displacement machines is not new as internal combustion engines have been tuned for a long time. However, the tuning procedures used for internal combustion engines cannot be applied directly to positive displacement compressors because of the following: (i) in compressors automatic suction and discharge valves are used which influence dynamic behavior and performance; (ii) any mass flow rate improvement does not necessarily translate into an improvement in energy efficiency since a corresponding, or higher, increase in power consumption may occur [1, 2]. Therefore, the problem of tuning a compressor is quite complex. It can, however, be stated simply as the process of increasing compressor efficiency through suitable modifications to the suction or discharge manifolds.

The purpose of this paper is to present a computer-aided analysis scheme for examining the tuning process; an example case of a two-cylinder refrigeration compressor is used to show this.

## 2. LITERATURE REVIEW

Only a few studies on compressor tuning have been found in the literature [2, 4–7], therefore relevant material on internal combustion engines are also reviewed here [1, 8–12]. The following conclusions relevant to air, gas, and refrigerant compressors can be drawn from this literature.

(1) Several tuning methods are based on producing a pressure resonance at the valves by using the Helmholtz resonator or the quarter-wave resonator approach [2, 4–10]. It has been shown that the working cylinder in engines may constitute the compliance element of a tuned Helmholtz resonator [8–10].



0022-460X/84/230475+14 $03.00/0 

(2) Some disagreement on the precise effect of suction tuning upon energy efficiency has been found. According to Laville and Soedel on engines [12] and Brablik on compressors [2], the energy efficiency of any tuned manifold cannot exceed the efficiency achieved without any manifold.
(3) All of the compressor tuning studies [2, 4–7] and most of the engine studies [8, 11, 12] have been restricted to single cylinder machines. In an experimental investigation on a multicylinder diesel engine [9], each cylinder was tuned separately with the assumption that during the intake opening other cylinders only offer "dead" volumes to the fluid flow. Dynamic coupling between the cylinders which leads to the wave interference mechanism is not accounted for.
(4) In previous experimental tuning studies on compressors generally ideal conditions have been assumed, such as unlimited working fluid availability, unrestrained valve motion, etc. [2, 4, 5].

## 3. SCOPE AND OBJECTIVES

### 3.1. SCOPE

For the performance of a compressor tuning study, an analytical approach is desired. An analytical approach is preferred over an experimental approach for the following reasons: (i) an analytical study can provide a systematic procedure rather than the trial and error experimental approach, (ii) an experimental study could be quite costly and time consuming, and further (iii) it is quite difficult to acquire a complete set of clear results experimentally because compressor performance is so sensitive to manifold geometry changes and working fluid conditions. Accurate and consistent manifold geometry and refrigerant conditions cannot be easily maintained during an entire experimental tuning study.

A computer simulation must be used as the analytical means of studying the compressor tuning process because closed form solutions are not possible. The computer simulation program and tuning procedure developed in this study are applicable to all practical manifolds and will be demonstrated using an example case.

### 3.2. OBJECTIVES

In this study, the effects of manifold gas pulsations and valving system dynamics upon compressor processes are to be investigated. To study this manifold back pressure effect, the following tasks will be performed.
(1) A computer simulation program will be developed to simulate a one- or two-cylinder positive displacement compressor which includes the manifold back pressure effect. This simulation program will include models of the following: piston drive kinematics, cylinder thermodynamics, fluid flow through the valves, valve dynamics, and manifold gas pulsations. Since the emphasis is on valve and manifold gas dynamics and their effect upon the basic thermofluid processes, the program developed here will model valve and manifold dynamics quite well while the remaining models are sufficient to enable reliable tuning results to be obtained. Since the tuning process requires repetitive running of the simulation program, all models will be simplified from well documented mathematical models [3, 13–19] as much as possible to reduce computation costs. Simplifications in models of valve and manifold gas dynamics are such to restrict validity of the simulation program to lower frequencies. However, since only the lower frequencies significantly affect the compressor processes, the validity of the simulation program for tuning studies should still be good. The program will be validated by comparing the results from it to results from a benchmark simulation [15] which is more sophisticated.

(2) A study of the effects of manifold back pressure upon compressor performance will be performed and tuning demonstrated with an example case. The example compressor is a two-cylinder reciprocating piston compressor with typical suction and discharge manifolds. The tuning study, using the simulation program described above, will be performed on the suction manifold which is symmetric about the cylinders. Variations in flow efficiency, energy efficiency, and suction manifold pressure pulsations will be shown to be dependent upon the acoustic behavior of the suction manifold. Experimental tuning data for the first acoustic natural frequency of such a suction manifold will be used for comparison with the simulation program results. Design guidelines for tuning compressor manifolds will then be discussed.

## 4. MATHEMATICAL MODELS

The computer simulation program is restricted to modeling a one- or two-cylinder reciprocating piston compressor in steady state operation, in which either a slider-crank mechanism or a scotch-yoke mechanism is used. Thermodynamic assumptions include ideal gas behavior and a polytropic cylinder process model. The model for valve motion consists of a single degree of freedom dynamic system excited by the instantaneous pressure differential across the valve. The manifold gas pulsations are described in the frequency domain by using acoustic plane wave theory, and the mean fluid flow effects, with the exception of damping, have been ignored. The dynamic valve model (only one degree of freedom) and the manifold gas pulsation model (only plane waves) are such that the overall simulation model is generally valid at lower frequencies. This frequency range of interest is limited to the first 10 harmonics of the running speed (approximately 3600 r.p.m.); thus, the range of interest is 0–600 Hz.

The mathematical models which follow are only those necessary for this tuning study and have been simplified as much as possible while still providing sufficient accuracy to give valid tuning results. More accurate and sophisitcated models are available [3, 13–19]; however, we wish to keep the models simplified in order to reduce computation costs.

### 4.1. COMPRESSOR PROCESSES

A typical two cylinder compressor is shown in Figure 1; operating variables are also shown (see the Appendix for the identification of symbols). The cylinder volume $V_c(\theta)$

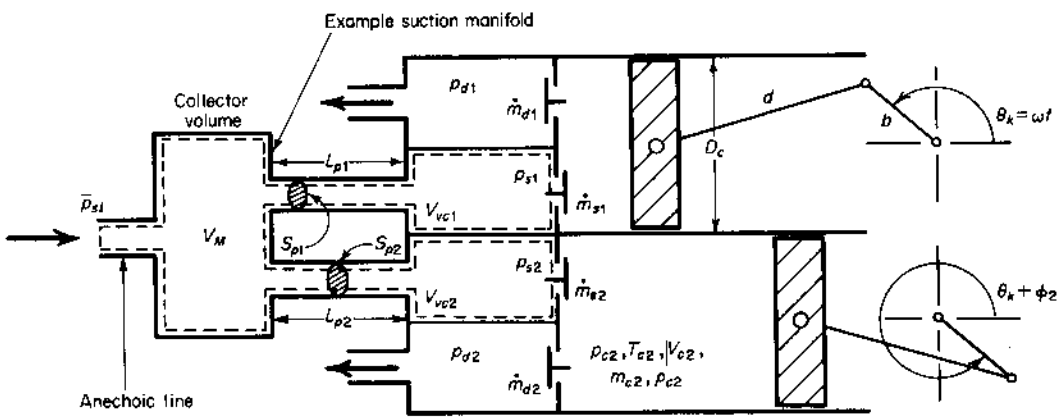


Figure 1. Schematic of example case: a two cylinder compressor and suction manifold.

for a slider-crank mechanism is given by

$$V_{ci}(\theta) = V_0 + (\pi/4) D_c^2 b \left[1 + \cos\theta + (d/b)\left(1 - \sqrt{1 - (b/d)^2 \sin^2\theta}\right)\right] \qquad i = 1, 2, \quad (1a)$$

$$\theta = \omega t + \phi_i. \quad (1b)$$

For a scotch-yoke mechanism the corresponding equation for cylinder volume is

$$V_{ci}(\theta) = V_0 + (\pi/4) D_c^2 b (1 + \cos\theta). \quad (2)$$

The cylinder process and equation of state are as follows:

$$p_{ci}(\theta) = p_0 [m_{ci}(\theta)/\rho_0 V_{ci}(\theta)]^a, \qquad p_{ci} V_{ci} = m_{ci} R T_{ci}, \qquad T_{ci}(\theta) = T_0 [p_{ci}(\theta)/p_0]^{(a-1)/a}. \quad (3, 4, 5)$$

The conservation of mass principle applied to the cylinder gives

$$m_{ci}(\theta) = m_{ci}(\theta_k) + \int_{\theta_k}^{\theta_{k+1}} [\dot{m}_{si}(\theta) - \dot{m}_{di}(\theta)]\, d\theta. \quad (6)$$

For the assumption of steady, isentropic flow of an ideal gas the mass flow rate $\dot{m}_{vi}$ to the valve throat is given as

$$\dot{m}_{vi}(\theta) = C_{Di}(\theta) A_{vi}(\theta) p_{ui}(\theta) \sqrt{2gk/[(k-1) R T_{ui}(\theta)][r_i(\theta)^{2/k} - r_i(\theta)^{(k+1)/k}]}, \quad (7a)$$

$$r_i = p_{vi}/p_{ui} \quad \text{if } r_i > r_c; \qquad r_i = r_c = [2/(k+1)]^{k/(k-1)} \quad \text{if } r_i \leqslant r_c. \quad (7b, c)$$

The equation of motion for the valve model is

$$d^2 y_{vi}(t)/dt^2 + 2\zeta_{rv}\omega_{rv}\, dy_{vi}(t)/dt + \omega_{rv}^2 [y_{vi}(t) - X_v] = [f_{vi}(t) + F_v]/m_{rv}, \quad (8)$$

where the valve force is

$$f_{vi}(t) = [p_{ui}(t) - p_{vi}(t)] B_{vi}(t). \quad (9)$$

### 4.2. MANIFOLD PULSATIONS

Gas pulsations in the manifolds cause the back pressure effects which influence valve motion and other compressor processes. Such interactions can most easily be handled in the frequency domain [16, 20]. The source function which excites the gas oscillations in the manifolds is the mass flow rate of the gas through the valves. Since the mass flow rate is a cyclic function in $t$ or $\theta$ one can express it in finite Fourier series form as

$$\tilde{\dot{m}}_{vi}(\theta_k) = \dot{m}_{vi}(0) + \sum_{n=1}^{N} |\tilde{\dot{m}}_{vi}(n\omega)| \exp j[n(\theta_k + \phi_i) + \psi_{vi}(n\omega)],$$

$$i = 1, 2; k = 0, 1, \ldots, M, \quad (10a)$$

$$\dot{m}_{vi}(0) = (2/M) \sum_{k=0}^{M} \dot{m}_{vi}(\theta_k), \quad (10b)$$

$$|\tilde{\dot{m}}_{vi}(n\omega)| = (2/M) \sqrt{\left[\sum_{k=0}^{M} \dot{m}_{vi}(\theta_k) \cos n(\theta_k + \phi_i)\right]^2 + \left[\sum_{k=0}^{M} \dot{m}_{vi}(\theta_k) \sin n(\theta_k + \phi_i)\right]^2},$$

$$n = 1, 2, \ldots, N, \quad (10c)$$

$$\psi_{vi}(n\omega) = \arctan\left\{\left[-\sum_{k=0}^{M} \dot{m}_{vi}(\theta_k) \sin n(\theta_k + \phi_i)\right] \Big/ \left[\sum_{k=0}^{M} \dot{m}_{vi}(\theta_k) \cos n(\theta_k + \phi_i)\right]\right\},$$

$$n = 1, 2, \ldots, N. \quad (10d)$$

From the mass flow rate, the acoustic volume velocity is determined:

$$\tilde{Q}(n\omega) = \tilde{m}_{vi}(n\omega)/\bar{\rho}_{vi}, \qquad n = 0, 1, 2, \ldots, N. \tag{11}$$

The acoustical impedances are calculated by using transfer matrix (or four-pole) descriptions of the continuous manifold sections. The four-pole theory for cascading linear acoustic elements is well developed, as has been shown by Rschevkin [19] and Singh [16]. For an arbitrary acoustic element, the relationship between acoustic variables at input (1) and output (2) can be given in terms of the four-pole and impedance matrices as

$$\begin{Bmatrix} \tilde{p}(\omega) \\ \tilde{Q}(\omega) \end{Bmatrix}_1 = \begin{bmatrix} \tilde{A}(\omega) & \tilde{B}(\omega) \\ \tilde{C}(\omega) & \tilde{D}(\omega) \end{bmatrix} \begin{Bmatrix} \tilde{p}(\omega) \\ \tilde{Q}(\omega) \end{Bmatrix}_2, \tag{12}$$

$$\begin{Bmatrix} \tilde{p}_1(\omega) \\ \tilde{p}_2(\omega) \end{Bmatrix} = \begin{bmatrix} \tilde{Z}_{11}(\omega) & \tilde{Z}_{12}(\omega) \\ \tilde{Z}_{21}(\omega) & \tilde{Z}_{22}(\omega) \end{bmatrix} \begin{Bmatrix} \tilde{Q}_1(\omega) \\ \tilde{Q}_2(\omega) \end{Bmatrix}. \tag{13}$$

Thus, the input and transfer impedance values can be determined as

$$\tilde{Z}_{11}(\omega) = \tilde{Z}_{22}(\omega) = \tilde{A}(\omega)/\tilde{C}(\omega), \qquad \tilde{Z}_{12}(\omega) = \tilde{Z}_{21}(\omega) = 1/\tilde{C}(\omega), \tag{14, 15}$$

where each impedance term is a complex quantity: i.e.,

$$\tilde{Z}_{ij}(\omega) = |\hat{Z}_{ij}(\omega)| \exp \mathrm{j}[\psi_{zij}(\omega)]. \tag{16}$$

The pulsating pressure at the valve exits can now be determined from

$$\underset{L\times 1}{\{\tilde{p}_{vi}(n\omega)\}} = \underset{L\times L}{[\tilde{Z}_{vij}(n\omega)]} \underset{L\times 1}{\{\tilde{Q}_{vi}(n\omega)\}}. \tag{17}$$

The valve exit pressure is defined by its finite Fourier series as [16, 20]

$$p_{vi}(\theta_k) = \bar{p}_{vi} + p_{vi}(0) + \sum_{n=1}^{N} |\tilde{p}_{vi}(n\omega)| \cos[n(\theta_k + \phi_i) + \beta_{vi}(n\omega)], \qquad k = 0, 1, \ldots, M. \tag{18}$$

Here $|\tilde{p}_{vi}(n\omega)|$ and $\beta_{vi}(n\omega)$ are computed from equation (17).

### 4.3. THERMOFLUID PERFORMANCE CHARACTERISTICS

The cyclic cylinder work $W_{ci}$, power required $P_{ci}$, cyclic suction mass flow rate $m_{si}$, volumetric efficiency $\eta_{vi}$, flow efficiency $\eta_{Fi}$ (an index of refrigeration capacity), and energy efficiency $\eta_{Ei}$ are computed in this study to evaluate compressor performance:

$$W_{ci} = \int_{V_{ci}(0)}^{V_{ci}(2\pi)} p_{ci}(\theta)\, \mathrm{d}V_{ci}(\theta) \quad \text{or} \quad W_{ci} = \sum_{k=0}^{M} p_{ci}(\theta_k)[V_{ci}(\theta_k + \delta/2) - V_{ci}(\theta_k - \delta/2)], \tag{19a, b}$$

$$P_{ci} = \omega W_{ci}/(2\pi\eta_M\eta_f), \qquad m_{si} = \int_0^{2\pi} \dot{m}_{si}(\theta)\frac{d\theta}{\omega} = \frac{\delta}{\omega}\sum_{k=0}^{M} \dot{m}_{si}(\theta_k), \tag{20, 21}$$

$$\eta_{vi} = \int_0^{2\pi} \dot{m}_{si}(\theta)\frac{\mathrm{d}\theta}{\omega}\left[\frac{2}{b\pi D_c^2\bar{\rho}_{si}}\right] \quad \text{or} \quad \eta_{vi} = \frac{2\delta}{\pi\omega b D_c^2\bar{\rho}_{si}}\sum_{k=0}^{M} \dot{m}_{si}(\theta_k), \tag{22a, b}$$

$$\eta_{Fi} = m_{si}h_I, \qquad \eta_{Ei} = \frac{m_{si}h_I}{P_{ci}}. \tag{23, 24}$$

Here $h_I$ is the enthalpy change during isentropic compression.

## 5. SIMULATION VALIDATION

No experimental data was available for validating the simulation program developed in this study so validation comparisons are based upon results from a benchmark simulation program [15] which is somewhat similar but more sophisticated. The following additional models are included in the benchmark simulation: (i) a motor model, (ii) real fluid properties, and (iii) energy losses at the cylinder (an accurate heat transfer model and fluid leakage past the piston).

The benchmark simulation has been found to be very accurate as all predictions it made were within ±4% of the measurements [15]. The comparisons between our simulation and the benchmark in Figures 2–4 are all for cylinder 1. All comparisons of the cyclic variables match very well with the results of the benchmark simulation. The suction valve chamber pressure line spectra in Figure 4 compare well, showing the same general shapes for both magnitude and phase. The discrepancies of up to about 5 dB in the magnitude harmonics are due to the gas density inaccuracy associated with the ideal gas assumption.

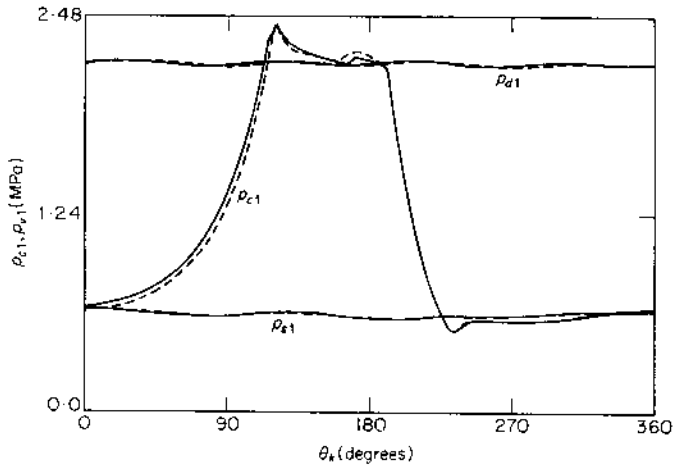


Figure 2. Cyclic pressure validation. ——, Benchmark simulation: - - -, this simulation.

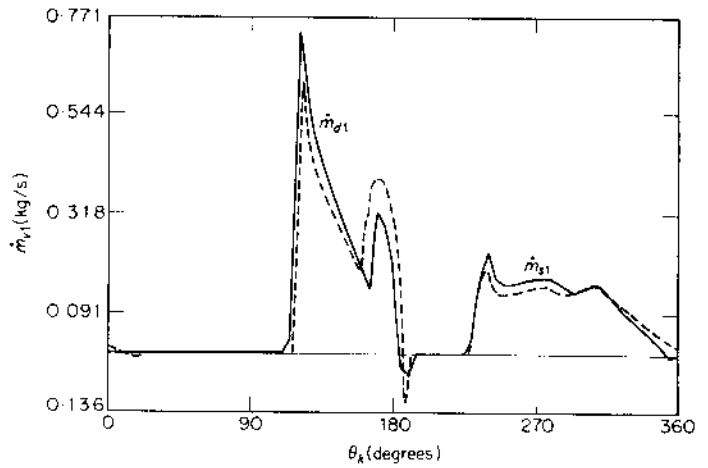


Figure 3. Cyclic mass flow rate validation. ——, Benchmark simulation; - - -, this simulation.

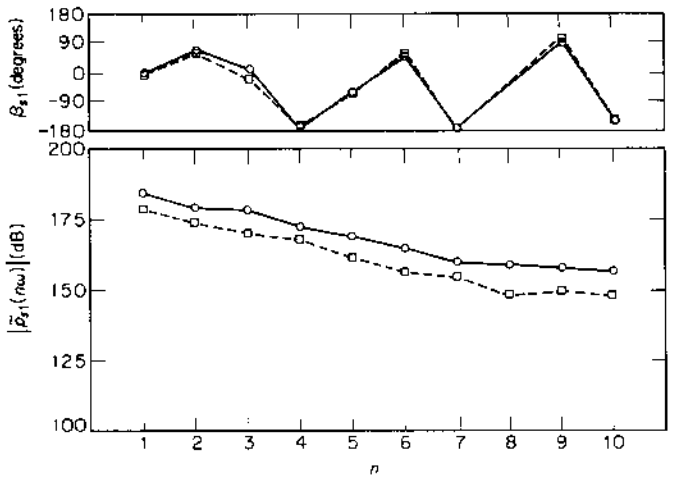


Figure 4. Suction manifold pressure line spectra validation. ——, Benchmark simulation: – – –, this simulation.

TABLE 1

*Comparison of thermofluid performance indices*

| Performance characteristic | Benchmark program [15] | Program used in this study | |
|---|---|---|---|
| | | Two-cylinder model | One-cylinder model |
| $W_{c1}$ (J/rev) | 34·50 | 32·35 | 33·11 |
| Ideal $W_{c1}$ (J/rev) | 30·67 | 30·33 | 30·66 |
| $\eta_{V1}$ (%) | 85·4 | 88·1 | 90·9 |
| $\eta_{F1}$ (kW) | 6·834 | 6·523 | 6·717 |
| $\eta_{E1}$ (kW/kW) | 3·442 | 3·504 | 3·526 |

A comparison of the thermofluid performance indices is given in Table 1. The values shown compare quite well, in view of the differences between the programs. All values are within 7% of the benchmark program.

## 6. EXAMPLE CASE

### 6.1. MANIFOLD GEOMETRY

The schematic in Figure 1 of a two-cylinder compressor shows that the suction manifold used in this study is symmetric between the cylinders. The kinematic phasing between piston 2 and piston 1 is 180°. In terms of manifold geometry, symmetry means $l_{p1} = l_{p2}$, $S_{p1} = S_{p2}$, and $V_{vc1} = V_{vc2}$.

To tune the suction manifold, it is desirable to investigate the effect of changing the geometrical variables ($l_p$, $S_p$, $V_{vc}$, $V_m$) upon corresponding changes in the compressor performance indices such as flow efficiency $\eta_F$, energy efficiency $\eta_E$, and manifold pressure pulsations $\Delta p_{sv}$.

### 6.2. PERFORMANCE INDICES

The performance indices presented for the tuning study are for cylinder 1 of the two-cylinder model. These performance indices are presented in non-dimensional form

and plotted versus a frequency ratio in order to make the curves very general and to illustrate better significant improvements in performance. The non-dimensional performance indices are

$$\eta_F^* = \eta_F / \eta_F^\circ, \qquad \eta_E^* = \eta_E / \eta_E^\circ, \qquad \Delta p_{sv}^* = \Delta p_{sv} / \bar{p}_{sl}, \qquad \Delta p_{sv} = \max [p_s(\theta)] - \min [p_s(\theta)], \tag{25}$$

where $\eta_F^\circ$ and $\eta_E^\circ$ are the values of the reference case, $\Delta p_{sv}$ is the peak-to-peak suction pressure, and $\bar{p}_{sl}$ is the average suction line pressure. It should be noted that these performance indices are often examined by the designer as a part of the efficiency improvement and pulsation control studies.

The abscissa of the graphs is the frequency ratio $\xi_r = f_r / f_0$, where $f_r$ is the $r$th acoustic natural frequency of the manifold and $f_0$ is the crank frequency. The acoustic natural frequencies of the manifolds are determined by locating the frequencies of the undamped resonant peaks in the impedance magnitude spectra. Mathematically, the peaks can be indicated in an impedance spectrum by the following:

$$Z(\omega) \to \frac{1}{(\omega - \omega_1)(\omega - \omega_2) \cdots (\omega - \omega_r) \cdots}. \tag{26}$$

Over the frequency range of interest, one finds two natural frequencies, $\omega_1$ and $\omega_2$. These can be related to the geometry of the symmetric manifold system by using a lumped parameter analysis [18]:

$$\omega_1 \simeq c\sqrt{S_p / l_p V_{vc}}, \qquad \omega_2 \simeq c\sqrt{(S_p / l_p)[(1/V_{vc}) + (2/V_M)]}. \tag{27}$$

Associated first and second mode shapes can be found in reference [18].

## 7. RESULTS AND DISCUSSION OF EXAMPLE CASE

Figures 5, 6 and 7 show the graphs of $\eta_F^*$, $\eta_E^*$, and $\Delta p_{sv}^*$, respectively, versus $\xi_1$ when fluid-induced damping is included in the manifold model; for damping description see references [17] and [20]. In a few studies [6, 7] graphs have been shown somewhat similar to that in Figure 5 for flow efficiency, but no references have been found to have graphical

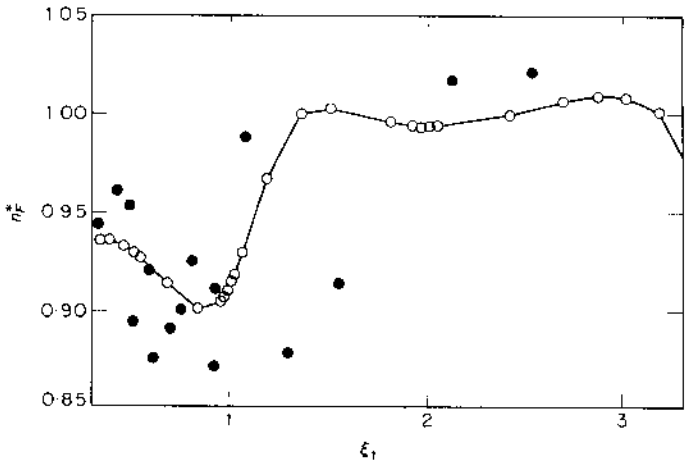


Figure 5. Flow efficiency versus first acoustic natural frequency (by $l_p$ variation). O—O, Simulation; ●, experimental data.

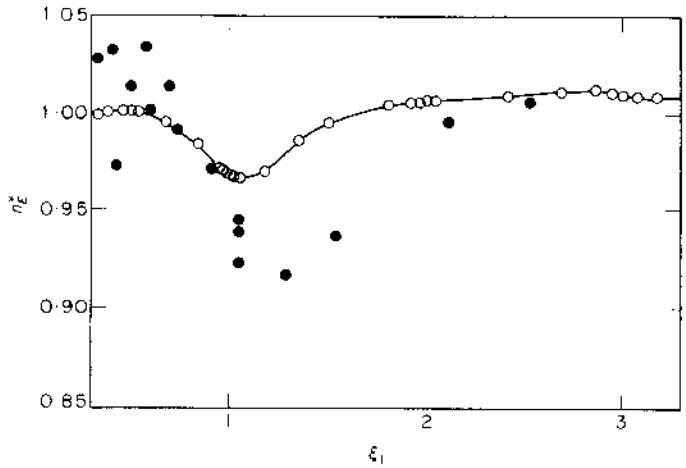


Figure 6. Enrgy efficiency verus first acoustic natural frequency (by $l_p$ variation). O—O, Simulation; ●, experimental data.

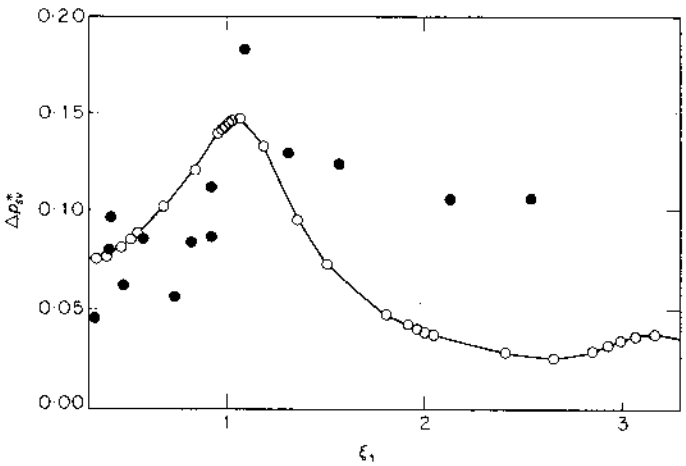


Figure 7. Peak-to-peak pressure pulsations at the suction valve versus first acoustic natural frequency (by $l_p$ variation). O—O, Simulation; ●, experimental data.

results for energy efficiency as in Figure 6. The first point to note in the simulation data on these graphs is the large change in the performance indices $\eta_F^*$, $\eta_E^*$ $\Delta p_{sv}^*$ around $\xi_1 = 1$ and the definite change in these indices throughout the range of $\xi_1$ shown. This is because the first harmonic of $f_0$ excites the first mode of manifold acoustics at $\xi_1 = 1$, and the third harmonic at $\xi_1 = 3$ also excites the first mode somewhat, but considerably less than the first harmonic. The graph in Figure 7 for suction pressure pulsations clearly shows this as the pressure pulsations are very large when the first mode is excited at $\xi_1 = 1$, and are still noticeable at $\xi_1 = 3$. In fact, as Singh and Soedel [18] have shown previously, the odd harmonics of the running speed $f_0$ excite the first mode of pressure pulsations in a symmetric two-cylinder manifold. However, the harmonics above the third do not generally have a significant effect upon compressor performance, as shown in some previous studies [6, 7, 16, 20]. It is apparent that maximum values of $\eta_F^*$ and $\eta_E^*$, and a minimum value of $\Delta p_{sv}^*$, can be obtained for a certain value of $\xi_1$. In this study for this particular compressor

design, $\xi_1$ in the range 2·8–2·9 optimizes the performance indices. Another significant point to observe in Figures 5, 6 and 7 is how the experimental data compares to the simulation data; the comparison is reasonably good as both the magnitude and overall shape are in agreement. It should be pointed out that the experimental data was collected over a long period of time. During this length of time, it was difficult to maintain the same compressor design and operating conditions. Also, the compressor was very sensitive to the dimension of $l_p$ (as demonstrated here), which was difficult to maintain. Thus, there is considerable uncertainty associated with the experimental data.

Figures 8 and 9 are graphs of $\eta_F^*$ and $\eta_E^*$, and $\Delta p_{sv}^*$, respectively, versus $\xi_2$ when fluid-induced damping is included in the manifold model. The respective shapes are the same as for Figures 5, 6 and 7 since the same performance data was obtained for each manifold variation described by both $f_1$ and $f_2$. Now one can see that the even harmonics, especially the second and the sixth, excite the second mode of gas pulsations in the

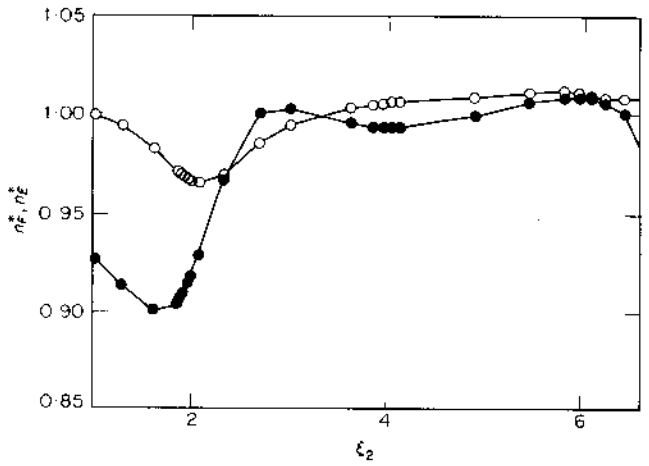


Figure 8. Flow and energy efficiency versus second acoustic natural frequency (by $l_p$ variation). ●—●, Flow efficiency; ○—○, energy efficiency.

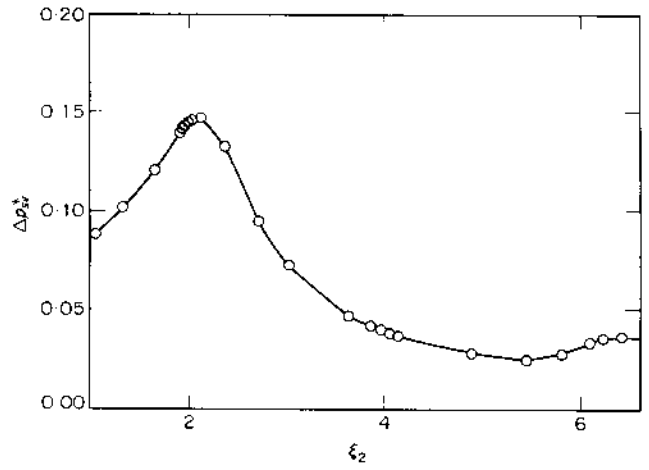


Figure 9. Peak-to-peak pressure pulsations at the suction valve versus second acoustic natural frequency (by $l_p$ variation).

manifold, as previously determined by Singh and Soedel [18]. Here $\xi_2$ can be chosen to be in the range of about 5·8–6·0 to maximize $\eta_F^*$ and $\eta_E^*$, while $\Delta p_{sV}^*$ is nearly a minimum here. No experimental data for tuning the second mode of the manifold is available for comparison with the simulation data.

Complete sets of graphs for variations of $S_p$ and $V_{vc}$ are documented in reference [20]; they show similar results to those presented here for the $l_p$ variations.

## 8. DESIGN IMPLICATIONS

The acoustic characteristics of a manifold definitely affect the thermofluid performance of a positive displacement compressor; large variations in flow and energy efficiencies and manifold pressure pulsations are found as the acoustic natural frequencies of the manifold are varied. Thus, the manifold must be tuned properly in any compressor design study. Typical steps towards tuning a compressor may be as follows: (i) monitor the performance of a compressor design as the geometry of the manifold (and, therefore, the acoustic natural frequencies) is varied; (ii) graphs similar to those in section 7 can be constructed to show the change in performance indices as the natural frequencies are varied; then (iii) a manifold geometry can be chosen which is characterized by the acoustic natural frequencies that give optimal performance.

A designer should be aware of the following points regarding the tuning process.

(1) For the example case of a symmetric two-cylinder suction manifold, odd crank frequency harmonics of the mass flow rate (or volume velocity) excite the first acoustic mode, and even harmonics excite the second acoustic mode. If excitation of these modes results in undesirable performance, as shown in section 7, they should be avoided by selecting a manifold geometry such that the acoustic natural frequencies do not coincide with the lower harmonics of the excitation (crank) frequency.

(2) The manifold geometry not only should be specified to avoid poor compressor performance, it should be suitably selected so as to optimize compressor performance. The tuning results have clearly shown this for the example case used in this study; the first natural frequency can be chosen such that the ratio $\xi_1 (= f_1/f_0)$ is in the range 2·8–2·9, and the second natural frequency can be chosen such that the ratio $\xi_2 (= f_2/f_0)$ is in the range 5·8–6·0 to optimize the compressor performance indices. The flow and energy efficiency results show that these two efficiencies may not vary in the same way with corresponding changes in the manifold acoustic natural frequencies. Therefore, one must perform a tuning study to determine which frequency ratios result in the largest values of both flow and energy efficiency while pressure pulsations are acceptably low. However, sometimes flow efficiency can be increased easily by selecting a larger stroke, then the frequency ratios can be chosen solely on energy efficiency and pressure pulsations.

## 9. CONCLUDING REMARKS

This study has initiated a basic understanding of the compressor tuning processes as performance indices have been found to be strongly dependent upon manifold acoustic natural frequencies. In a subsequent publication, we will describe manifold acoustics in an analytical function form which can be related to the compressor performance indices [21].

Specific areas where further research should be directed are the following: (i) development of more accurate models for compressor components and processes which influence the steady compressor operation (these models could include multi-degree-of-freedom valve motion, mean flow effects, finite amplitudes, and non-linear effects in the manifold

passages); (ii) development of a computer-based command program to perform the tuning study with optimization routines to find the optimum manifold designs; (iii) examination of other available results of tuning studies on different machines, by using the approach taken here.

## ACKNOWLEDGMENTS

We would like to acknowledge the much appreciated financial support of Copeland Corporation, Sidney, Ohio, and the assistance of Fran Simpson and Young-In Moon.

## REFERENCES

1. W. SOEDEL 1978 *Short Course Text, Purdue University.* Gas pulsations in compressor and engine manifolds.
2. J. BRABLIK 1974 *Proceedings of the Second Purdue Compressor Technology Conference,* 151–158. Computer simulation of the working process in the cylinder of a reciprocating compressor with piping system.
3. R. SINGH 1975 *Ph.D. Thesis, Purdue University.* Modeling of multicylinder compressor discharge systems.
4. F. K. BANNISTER 1958 *Proceedings of the Institution of Mechanical Engineers* **117**, 375–397. Induction ramming of small high speed air compressor.
5. R. A. STEIN and J. A. EIBLING 1962 *Proceedings of the Xth International Congress of Refrigeration, Washington, D.C.,* 191–207. Improving compressor performance by discharge tuning.
6. H. A. JASPERS 1969 *Proceedings of the XIIth International Congress of Refrigeration, Madrid, Spain, Paper No.* 3.54, 839–846. Special suction lines influencing the volumetric efficiency of reciprocating compressors.
7. S. TOUBER and H. J. BLANKESPOOR 1975 *Proceedings of the XIVth International Congress of Refrigeration, Moscow, U.S.S.R., Paper No. B*2.16, 773–784. Hybrid computer simulation of the effects of suction and discharge pressure pulsations in a reciprocating compressor.
8. H. W. ENGLEMAN 1953 *Ph.D. Thesis, University of Wisconsin.* Surge phenomena in engine scavenging.
9. W. M. EBERHARD 1971 *M.Sc. Thesis, The Ohio State University.* A mathematical model of ramcharging intake manifolds for four-stroke diesel engines.
10. A. L. SCHWALLIE 1972 *M.Sc. Thesis, The Ohio State University.* Verification of a mathematical model for intake manifold design.
11. D. C. KARNOP, H. A. DWYER and D. L. MARGOLIS 1975 *Society of Automotive Engineers Paper No.* 750708. Computer prediction of power and noise for two-stroke engines with power tuned, silenced exhausts.
12. F. LAVILLE and W. SOEDEL 1978 *Journal of the Acoustical Society of America* **63,** (S-1). Thoughts on the effect of acoustic back pressures on engine performance.
13. W. SOEDEL 1972 *Ray W. Herrick Laboratories, Purdue University.* Introduction to computer simulation of positive displacement type compressors.
14. W. SOEDEL and S. WOLVERTON 1974 *Ray W. Herrick Laboratories, Purdue University.* Anatomy of a compressor simulation program.
15. M. SCHARY, F. SCHEIDEMAN and R. SINGH 1978 in *Simulation of Energy Systems* (Editor K. E. F. Watt), Part 2, Chapter 17, 173–181. La Jolla, California: The Society for Computer Simulation. Energy and pressure pulsation predictions for refrigeration compressors.
16. R. SINGH and W. SOEDEL 1979 *Journal of Sound and Vibration* **63,** 125–143. Mathematical modeling of multicylinder compressor discharge system interactions.
17. R. SINGH and W. SOEDEL 1978 *Journal of Sound and Vibration* **57,** 449–452. Assessment of fluid-induced damping in refrigeration machinery manifolds.
18. R. SINGH and W. SOEDEL 1979 *Journal of Sound and Vibration* **64,** 387–402. Interpretation of gas oscillations in multicylinder fluid machinery manifolds by using lumped parameter descriptions.
19. S. N. RSCHEVKIN 1963 *A Course of Lectures on the Theory of Sound.* New York: McMillan Co.
20. J. J. NIETER 1983 *M.Sc. Thesis, The Ohio State University.* A computer simulation and modal analysis study of compressor manifolds and tuning phenomena.
21. J. J. NIETER and R. SINGH 1982 *Journal of the Acoustical Society of America* **72,** 319–326. Acoustic modal analysis experiment.

## APPENDIX: LIST OF SYMBOLS

| | |
|---|---|
| $a$ | polytropic constant |
| $A, B, C, D$ | fourpole matrix elments |
| $A$ | flow area |
| $b$ | slider-crank length |
| $B$ | force area |
| $c$ | speed of sound |
| $C$ | coefficient of discharge |
| $d$ | slider-crank connecting rod length |
| $D$ | bore diameter |
| $f$ | frequency (Hz) |
| $F$ | preload |
| $g$ | gravitational constant |
| $h$ | enthalpy |
| j | imaginary number, $=\sqrt{-1}$ |
| $k$ | ratio of isentropic specific heat capacities |
| $l$ | length |
| $L$ | number of cylinders in compressor model |
| $m$ | mass |
| $M$ | number of discrete crank angle positions per cycle, $=2\pi/\delta$ |
| $m$ | mass flow rate |
| $n$ | harmonic number |
| $N$ | total number of harmonics in frequency analysis |
| $p$ | pressure |
| $P$ | power |
| $Q$ | acoustic volume velocity |
| $r$ | pressure ratio |
| $R$ | gas constant |
| $S$ | cross-sectional area |
| $t$ | time |
| $T$ | temperature |
| $V$ | volume |
| $W$ | cyclic work |
| $X$ | free lift |
| $y$ | valve displacement |
| $Z$ | acoustic impedance |
| $\beta$ | valve exit pressure phase angle |
| $\delta$ | crank angle increment |
| $\zeta$ | damping ratio |
| $\eta$ | efficiency |
| $\theta$ | crank angle |
| $\xi$ | frequency ratio |
| $\rho$ | density |
| $\phi$ | kinematic phase angle |
| $\psi$ | mass flow rate phase angle |
| $\omega$ | frequency (rad) |

*Subscripts*

| | |
|---|---|
| 0 | reference state (mean suction line condition) |
| 1 | cylinder; acoustic input position |
| 2 | cylinder; acoustic output position |
| $c$ | cylinder |
| $d$ | discharge |
| $D$ | discharge coefficient |
| $E$ | energy |
| $f$ | friction |
| $F$ | flow (a refrigeration capacity index) |
| $i$ | cylinder index |
| $I$ | isentropic |

| | |
|---|---|
| $j$ | cylinder index |
| $k$ | discrete crank angle index |
| $l$ | line |
| $M$ | motor |
| $n$ | harmonic index |
| $r$ | natural mode of oscillation |
| $s$ | suction |
| $u$ | upstream |
| $v$ | valve |
| $Z$ | impedance |

*Superscripts*

| | |
|---|---|
| $\tilde{}$ | complex quantity |
| $\bar{}$ | average quantity |
| { } | column vector |
| [ ] | square matrix |